Journal of Nonlinear Optical Physics & Materials
Vol. 25, No. 4 (2016) 1650047 (14 pages)

DOI: 10.1142/S0218863516500478

World Scientific
www.worldscientific.com

Coherent states and localization in a quantized discrete NLS lattice

R. Martinez-Galicia

Departamento de Matemáticas,
Facultad de Química,
Universidad Nacional Autónoma de México,
04510 Cd. México, México

Panayotis Panayotaros

Departamento de Matemáticas y Mecánica,
Instituto de Investigaciones en Matemáticas Aplicadas y en Sistemas,
Universidad Nacional Autónoma de México,
Apdo. Postal 20–126, 01000 Cd. México, México
panos@mym.iimas.unam.mx

Received 15 September 2016

We study the evolution of a quantum discrete nonlinear Schrödinger (DNLS) system using as initial conditions coherent states corresponding to points in the vicinity of breather solutions of the classical system. We consider various examples of stable and unstable breathers and examine the distance between exactly evolved states and coherent states with parameters that evolve according to classical dynamics. Initial conditions near stable breathers and their vicinity are seen to lead to recurrences to small distances between the two evolving states. Similar recurrences are not observed for initial conditions near unstable breathers.

Keywords: Discrete NLS; quantum DNLS; breathers; coherent states.

1. Introduction

The cubic discrete nonlinear Schrödinger (DNLS) equation in a one-dimensional lattice appears in many problems of physics where we have a combination of nonlinearity, discrete and spatial inhomogeneity effects. Moreover, as problems on nonlinear lattices often involve microscopic systems, quantum effects can be important. For example, in the study of small molecules, the DNLS equation has proven to be a simple and useful model for the calculation of molecular anharmonic vibrational spectra where quantum effects play an important role.[1–3] Also, the study of various low-dimensional materials with applications in the fields of, for example, energy and catalysis, are important for the understanding of the thermodynamic and transport properties of various materials. This study requires an understanding of the dynamics of nonlinear excitations, such as solitons and breathers, in both classical and quantum context.[4,5] On the other hand,

theoretical studies of the dynamics of a Bose–Einstein condensate trapped in optical lattice also use the DNLS equation as a model. The control achieved in the Bose–Einstein condensate opens the possibility of a new generation of devices at the nanoscale level.[6] Another field of applications is that of superconducting circuits used in quantum computing, modeled by coupled nonlinear oscillators that exhibit localized nonlinear vibration modes. As superconducting circuits are increasingly made smaller, the behavior of these nonlinear circuits starts to include quantum effects and the comparison of classical and quantum dynamics becomes interesting.[7]

These applications motivate the study of finite nonlinear lattices in the quantum regime. A basic question is also the dependence of the classical and quantum dynamics on the geometry of the lattice, e.g., the number of sites. In quantum systems, the DNLS appears as a mean field approximation and a general question is the quantum evolution from states that can be somehow related to classical initial conditions with interesting dynamical properties.

In the present work, we are specifically interested in the classical dynamics near spatially localized solutions of the DNLS and map points in the classical phase–space to quantum states using coherent states. In particular, we study the quantum evolution from Glauber and SU(f) coherent states,[11–15] see Sec. 3, that correspond to points near breather orbits of the DNLS.[8] The quantum evolution is generated by a Hamiltonian operator obtained from the DNLS via bosonic quantization,[16–18] see Sec. 2. Breather solutions, see Sec. 2, are here interesting mainly as examples of solutions with well-defined spatial localization.[19–21] To quantify the relation between classical and quantum dynamics, we examine the difference between the exactly evolved quantum state and a coherent state with parameters that evolve by classical dynamics.[22] Such "classically evolving coherent states define an alternative, *a priori* non-exact, but possibly approximate, evolution rule, see Refs. 14, 23 and 24.

Our main result is the observation of cases of recurrence of relatively small values of the distance between the two evolution rules. This recurrence is seen for classical initial conditions that are in the vicinity of stable breathers and suggest that the notion of localization of coherent states corresponding to such breathers is recurrent under the quantum evolution. For initial conditions in the vicinity of unstable breathers, we do not see similar recurrences. Rather, the distance between the exact and the classically evolved coherent states increases rapidly and fluctuates slightly around a large average, without any recurrence to significantly smaller values.

Note that the classically evolved coherent states are known to approximate well the exact quantum evolution for large number of quanta and small nonlinearity.[15,25–27] They are also exact solutions of linear systems.[11,12] Our study concerns parameter regimes far from these limits, and is especially relevant to the nonlinear localization regime where the intersite coupling is small ("the anticontinuous limit"[19]).

The phenomena presented here concern a lattice with five sites and corroborate similar observations made on the three site DNLS.[22] Using more sites is useful but also more computationally expensive, but a small increase in the lattice sites may bring us closer to some effects seen in lattices of hundreds of sites that may be relevant for some applications. In the present study, our goal is also to examine unstable breathers localized at two consecutive sites, argued to have some possible importance for the global dynamics of finite DNLS latices in Ref. 33, see also Ref. 22. In the trimer, these solutions are affected by the fact that one of the peaks is at the edge of the lattice. The five-site problem avoids that problem, is seen to have somewhat different dynamics, see Sec. 3, and may be more representative of what we should see in larger lattices. We are currently working towards a possible explanation of the recurrences and the differences between trajectories starting near stable and unstable breathers, see Secs. 3 and 4 for some remarks.

2. Discrete NLS Equation and Its Quantization

We consider a finite set of anharmonic oscillators evolving under the cubic DNLS equation

$$\frac{du_j}{dt} = -i\delta(\Delta u)_j - 2i|u_j|^2 u_j, \tag{2.1}$$

where $u_j \in \mathbb{C}$ is the complex amplitude of the oscillator at the lattice site j, $j \in \{1, \ldots, f\}$, and δ is a real number. The discrete Laplacian Δ is defined by

$$\begin{aligned} &(\Delta u)_j = u_{j+1} + u_{j-1} - 2u_j, \quad j = 2, \ldots, f-1, \\ &(\Delta u)_1 = u_2 - 2u_1, \quad (\Delta u)_f = u_{f-1} - 2u_f, \end{aligned} \tag{2.2}$$

a discrete analogue of Dirichlet boundary conditions. System (2.1) can be written as a Hamiltonian system

$$\frac{du_j}{dt} = -i\frac{\partial H}{\partial u_j^*}, \quad j = 1, \ldots, f, \tag{2.3}$$

where the Hamiltonian H is given by

$$H = -\delta\left(\sum_{j=1}^{f-1} |u_{j+1} - u_j|^2 + |u_1|^2 + |u_f|^2\right) + \sum_{j=1}^{f} |u_j|^4. \tag{2.4}$$

Another conserved quantity is the power $P = \sum_{j=1}^{f} |u_j|^2$. Its conservation corresponds to the invariance of H under global phase change.

A *breather* solution of (2.1) is a periodic solution of the form

$$u_j = e^{-i\omega t} A_j \tag{2.5}$$

with ω real, and $A = [A_1, \ldots, A_f] \in \mathbb{C}^f$ independent of time t.

Breather solutions are interesting for many reasons, they are for instance relative equilibria, and critical points of the energy for fixed power,[20] e.g., breathers that

are isolated from local extrema of the energy are linearly and nonlinearly (orbitaly) stable.[33] Their global properties and dynamics have been especially studied for the $f = 3$ ("trimer") system.[28–33] Breathers are also examples of solutions exhibiting spatial localization, e.g., for $|\delta| \to 0$ we can have breathers with $|A_j|$ of $O(\delta)$, and $O(1)$, respectively, in complementary sets of sites, see Refs. 19, 21 and 32.

To compute and analyze breathers, we substitute (2.5) in (2.1) to obtain that the A_j and ω satisfy the system of nonlinear equations,

$$-\omega A_j = -\delta(\Delta A)_j - 2|A_j|^2 A_j, \quad \sum_{j=1}^{f} |A_j|^2 = C, \quad j = 1, \ldots, f \tag{2.6}$$

for a fixed C. Breather solutions are computed by solving (2.6) numerically. The linear stability analysis of breather solutions is performed by introducing a disturbance $R_j(t)$ to the solution of (2.6). Considering (2.1) with $u_j = e^{-i\omega t}(A_j + R_j(t))$, using the fact that A_j, ω satisfy (2.6), and neglecting quadratic and higher order terms in $R_j(t)$, we obtain an autonomous system of linear differential equations for the $R_j(t)$. The eigenvalues of the matrix determine the linear stability of the breather solutions. The literature on the stability of breathers is extensive, see e.g., Refs. 10 and 21.

To define a quantum version of the above equations, we follow the standard (bosonic) quantization rules, see e.g., Refs. 16–18. Specifically, let V be the complex span of the *occupation number* basis elements $|n_1, n_2, \ldots, n_f\rangle$, where $n_1, \ldots, n_f \geq 0$. The $|n_1, \ldots, n_f\rangle$ are also assumed to form an orthonormal basis, satisfying

$$\langle m_f, \ldots, m_1 | n_1, \ldots, n_f \rangle = \delta_{m_1 n_1}, \ldots, \delta_{m_f n_f} \tag{2.7}$$

with $\delta_{m_i n_j}$, the Kronecker delta.

Under quantization, the amplitudes of the complex modes u_j^* y u_j of a model such as (2.1) are mapped to the bosonic creation and annihilation operators, $B_j^\dagger$ and B_j, $j = 1, \ldots, f$, defined by their action on the basis vectors as

$$\begin{aligned} B_j^\dagger |n_1, n_2, \ldots, n_j, \ldots, n_f\rangle &= \sqrt{n_j + 1}\, |n_1, n_2, \ldots, n_j + 1, \ldots, n_f\rangle, \\ B_j |n_1, n_2, \ldots, n_j, \ldots, n_f\rangle &= \sqrt{n_j}\, |n_1, n_2, \ldots, n_j - 1, \ldots, n_f\rangle \quad \text{if } n_j > 0, \\ B_j |n_1, n_2, \ldots, 0, \ldots, n_f\rangle &= 0 |n_1, n_2, \ldots, 0, \ldots, n_f\rangle. \end{aligned} \tag{2.8}$$

Using these definitions, we also define the quantized Hamiltonian operator $\hat{H}$ by

$$\hat{H} = (1 - 2\delta) \sum_{j=1}^{f} B_j^\dagger B_j + \sum_{j=1}^{f} B_j^\dagger B_j B_j^\dagger B_j + \delta \sum_{j=1}^{f} (B_j^\dagger B_{j+1} + B_j B_{j+1}^\dagger), \tag{2.9}$$

i.e., compare to the classical Hamiltonian of (2.4). Similarly P is "quantized" to the "number" operator $\hat{N}$, defined by $\hat{N} = \sum_{j=1}^{f} B_j^\dagger B_j$.

The dynamics of the quantum system is described by the Schrödinger equation

$$i \frac{\partial |\Psi(t)\rangle}{\partial t} = \hat{H} |\Psi(t)\rangle, \tag{2.10}$$

whose formal solution is $|\Psi(t)\rangle = e^{-iHt} |\Psi(0)\rangle$ with $|\Psi(0)\rangle$ the initial state.

Operators $\hat{N}$ and $\hat{H}$ commute and this implies that for any $n > 0$, the complex subspace V_n of states spanned by all $|n_1, \ldots, n_f\rangle$ satisfying $n_1 + \ldots n_f = n$ is invariant under the evolution of Schrödinger's equation. Equivalently, the matrix representation of $\hat{H}$ in the occupation number basis has a block diagonal form where each block, denoted by H_n, has entries $\langle\Psi_i|\hat{H}|\Psi_j\rangle$, with Ψ_i, Ψ_j elements of the occupation number basis of V_n. Numerical integration of (2.10), e.g., via numerical computation of the spectra and eigenvalues of $\hat{H}$ consider up to a finite number of these blocks. We can also consider the dynamics in any given V_n, corresponding to initial conditions of n quanta. Note that $\dim V_n = \frac{(n+f-1)!}{(f-1)!n!}$, i.e., we have factorial growth rates for the size of the blocks as we increase n and the lattice size f.

Calculations of the spectral properties of the quantized DNLS have been reported by many authors, and there are several possible definitions of spatial localization at the quantum level, Refs. 17, 25, 34–41 see Ref. 22 for a brief discussion. It appears that an intrinsically quantum notion of localization is not as natural for systems with translation symmetry.[38] In the next section, we turn instead to coherent states, quantum states that correspond in a natural way to points in the classical phase–space.

3. Coherent States and Quantum Evolution

Let $(\alpha) = (\alpha_1, \alpha_2, \ldots, \alpha_f) \in \mathbb{C}^f$. We define a Glauber coherent state $|(\alpha)\rangle$, $(\alpha) \in \mathbb{C}^f$, to be a normalized state in V that satisfies

$$\hat{B}_j|(\alpha)\rangle = \alpha_j|(\alpha)\rangle \tag{3.1}$$

for all $j = 1, 2, \ldots, f$. A normalized Glauber coherent state $|(\alpha)\rangle$ can be written explicitly as a linear combination of occupation number basis states, namely

$$\begin{aligned}|(\alpha)\rangle = {} & e^{-\frac{1}{2}(|\alpha_1|^2+|\alpha_2|^2+\cdots+|\alpha_f|^2)} \\ & \times \sum_{n_1=0}^{\infty}\sum_{n_2=0}^{\infty}\cdots\sum_{n_f=0}^{\infty}\frac{\alpha_1^{n_1}\alpha_2^{n_2}\cdots\alpha_f^{n_f}}{\sqrt{n_1!n_2!\cdots n_f!}}|n_1, n_2, \ldots, n_f\rangle,\end{aligned} \tag{3.2}$$

see e.g., Refs. 11 and 12. This expression leads to explicit formulas for projections to the subspaces V_n.

Let $\alpha(0) = (\alpha_1(0), \ldots, \alpha_f(0)) \in \mathbb{C}^f$ and consider a coherent state $|(\alpha(0))\rangle$. Fix any $n \geq 0$, and let

$$|\Psi_n(t)\rangle = e^{-iHt}P_n|(a(0))\rangle, \tag{3.3}$$

where P_n is the orthogonal projection to the subspace V_n. Then $|\Psi_n(t)\rangle$ describes the exact quantum evolution of $P_n|(\alpha(0))\rangle$ in the invariant subspace V_n.

We can also consider an alternative (non-exact, and possibly approximate) evolution rule for quantum states in the following way. Let $\alpha(t)$ be solution of Hamilton's equations (2.3) at time t with initial condition $\alpha(0)$ (as above). Also, let

$|(a(t))\rangle$ be the corresponding coherent state at any time t. Then define $|\tilde{\Psi}(t)\rangle$, and $|\tilde{\Psi}_n(t)$ by $|\tilde{\Psi}(t)\rangle = |(\alpha(t))\rangle$, and

$$|\tilde{\Psi}_n(t)\rangle = P_n|(\alpha(t))\rangle, \tag{3.4}$$

respectively. State (3.4) gives a "classical" approximation to the evolution of the projection of a coherent state.

The evolution rule of (3.4) can be derived using a variational Ansatz: coherent states form a set of trial functions parametrized by the variables of the classical phase–space, and Hamilton's equations are the necessary condition for the minimization of suitable functionals that vanish at the exact quantum evolution, see Refs. 14, 23 and 24. However, the assumption that a state that is initially a coherent state remains a coherent state at all times is not in general true. Furthermore, the variational derivation does not imply that the classically evolved coherent states are close to the exact states. The object of this paper to obtain further quantitative information on this alternative rule for breather solutions and for nearby initial conditions. Note that the classically evolved coherent states $|\tilde{\Psi}(t)\rangle$ approximate the quantum evolution in the so-called classical limit for the problem, see Refs. 15, 25 and 26, and are exact solutions of the linear problem.[11,12]

To compare the two rules of evolution above, we can measure the distance between the states $|\Psi_n(t)\rangle$ and $|\tilde{\Psi}_n(t)\rangle$, that is

$$D_n(t) = \inf_{\phi\in\mathbb{R}}\|e^{i\phi}|\Psi_n(t)\rangle - |\tilde{\Psi}_n(t)\rangle\|^2. \tag{3.5}$$

The orthogonality between the subspaces V_n implies that

$$\inf_{\phi\in\mathbb{R}}\|e^{i\phi}|\Psi(t)\rangle - |\tilde{\Psi}(t)\rangle\|^2 \geq \sum_{n=0}^{\infty}\inf_{\phi_n\in\mathbb{R}}\|e^{i\phi_n}|\Psi_n(t)\rangle - |\tilde{\Psi}_n(t)\rangle\|^2, \tag{3.6}$$

therefore the $D_n(t)$ of (3.5) for different n can be used to estimate from below the difference between the two evolution rules for the initial condition $|\Psi(0)\rangle = |(\alpha(0))\rangle$. Since the Glauber states are normalized, the $D_n(t)$ must vanish as $n \to \infty$.

Alternatively, we here consider the two evolutions for the *normalized* projections of $|\Psi(0)\rangle = |(\alpha(0))\rangle$ to each V_n. Such initial conditions correspond to quantum states with a definite number n of quanta. The difference between the two evolutions of the normalized state in V_n is then measured by

$$\overline{D}_n(t) = |||\Psi_n(0)\rangle||^{-2}D_n(t). \tag{3.7}$$

Normalized projected Glauber states are also known as SU(f) coherent states, see Refs. 14, 15 and 26.

We indicate our main observations on the evolution of $\overline{D}_n$ using three classical initial conditions in a lattice with $f = 5$ sites. We consider the case $\delta > 0$ in (2.1), i.e., the focusing (or attractive) case. We first consider a classical initial state

$$\mathcal{A}_1 = (0, 0, 1, 0, 0) \tag{3.8}$$

with energy completely localized at site $j = 3$ of the lattice. For $\delta = 0$, $\mathcal{A}_1$ is a stable breather. For $\delta \neq 0$, $\mathcal{A}_1$ is not a breather solution, but is still close to one if

$|\delta|$ is sufficiently small. We also consider one stable breather solution, one unstable breather, and an unstable breather solution of two-peaks in sites 2 and 3 of the lattice, $\mathcal{A}_2$, $\mathcal{A}_3$ and $\mathcal{A}_4$ below. Both satisfy (2.1) with $\delta = 0.3$, $C = 1$. The first solution has amplitude

$$\mathcal{A}_2 = (0.0230719, 0.153576, 0.975584, 0.153576, 0.0230719) \tag{3.9}$$

with frequency $\omega = 1.39798$. The breather $\mathcal{A}_2$ is linearly stable. The second solution is

$$\mathcal{A}_3 = (-0.663413, -0.0271497, 0.582775, 0.441421, 0.157056) \tag{3.10}$$

with $\omega = 0.292511$. The breather $\mathcal{A}_3$ is linearly unstable. The third solution, we consider

$$\mathcal{A}_4 = (0.16342, 0.687407, 0.684993, 0.173157, 0.0395882) \tag{3.11}$$

with $\omega = 0.715323$, has two peaks and is also unstable. In Ref. 33, it was argued that a breather solution with two consecutive peaks may be important for the global dynamics of the system, as it is likely to be the critical energy for the transition between a connected and non-connected energy surface at constant power, see also Ref. 22. The arguments of Ref. 33 were made for the $f = 3$ lattice and could apply to larger lattices. However, the dynamics of such a two-peak solution in the trimer may be affected by the fact that one of the peaks is at the edge of the lattice. Properties of two consecutive peak solutions for an $f = 5$ lattice with peaks at internal sites may be relevant to larger lattices.

We indicate some of the classical dynamics of the above breathers. Figure 1 uses $\mathcal{A}_1$ as initial condition, for $\delta = 0.3$. There is still localization of the energy at the site $j = 3$. Other sites have significantly smaller energy. However, this localization is lost once the value of the coupling constant δ increases, as seen in the case of $\delta = 0.5$. In Fig. 2, we show the evolution of the unstable breather $\mathcal{A}_3$. Note that after some time, $t \approx 30$, the breather is delocalized and energy is distributed in the rest of the sites.

We now consider the corresponding quantum evolution. According to Fig. 3, in the case of the classical initial condition $\alpha(0) = \mathcal{A}_1 = (0, 0, 1, 0, 0)$, and the

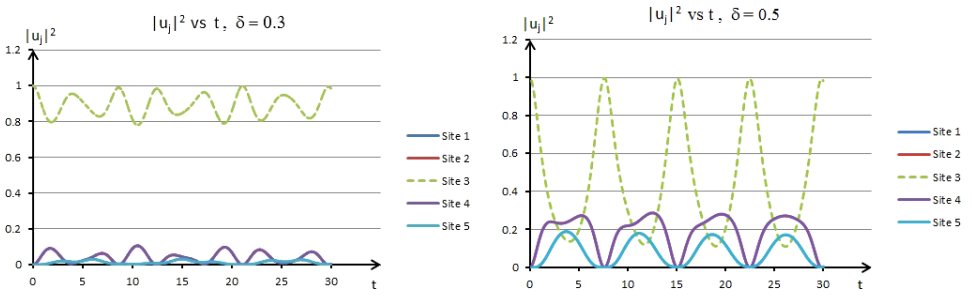

Fig. 1. Evolution of classical DNLS from initial state $\mathcal{A}_1 = (0, 0, 1, 0, 0)$ for $\delta = 0.3$ and $\delta = 0.5$.

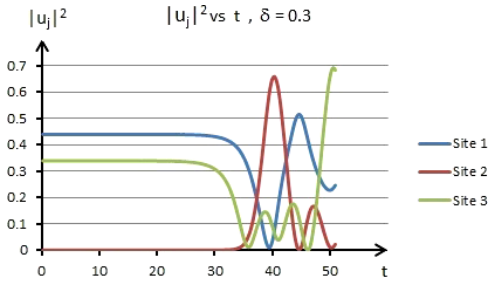

Fig. 2. Evolution of classical DNLS from initial condition $\mathcal{A}_3$, see (3.10), using $\delta = 0.3$. We show the amplitude of the first three sites.

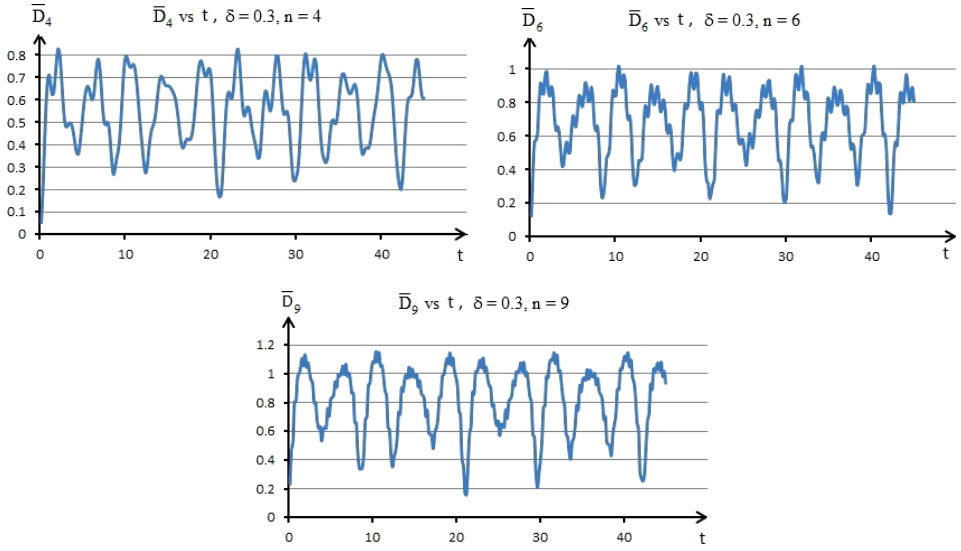

Fig. 3. $\overline{D}_n$ versus t, initial condition is the normalized projected Glauber state corresponding to classical state $\mathcal{A}_1$, see (3.8), for $n = 4$, 6 and 9 bosons, $f = 5$ sites, $\delta = 0.3$.

corresponding initial state $|(\alpha(0))\rangle$ you can see that the difference between states $|\Psi_n(t)\rangle$ and $|\tilde{\Psi}_n(t)\rangle$ go through minima at certain periods of time. Even though these minima are not zero, the figure suggests that states $|\Psi_n(t)\rangle$ y $|\tilde{\Psi}_n(t)\rangle$ are close at certain times. The time intervals between these recurring minima, and also their value also depend on the number of quanta n.

Figure 4 uses as classical initial condition $\alpha(0)$ the stable breather $\mathcal{A}_2$, and shows recurrences to comparable minima of $\overline{D}_n$. The time dependence of the distance is different from that of Fig. 3, and again depends on n.

Figure 5 is obtained using the coherent state corresponding to the classical initial condition $\alpha(0) = \mathcal{A}_3$, for $n = 4$, 6, and $n = 9$ bosons, respectively. The graph of $\overline{D}_n$ is unlike what we saw in the two previous examples. The distance increases rapidly to a value above 1.2 and remains in that range at all times. It therefore appears

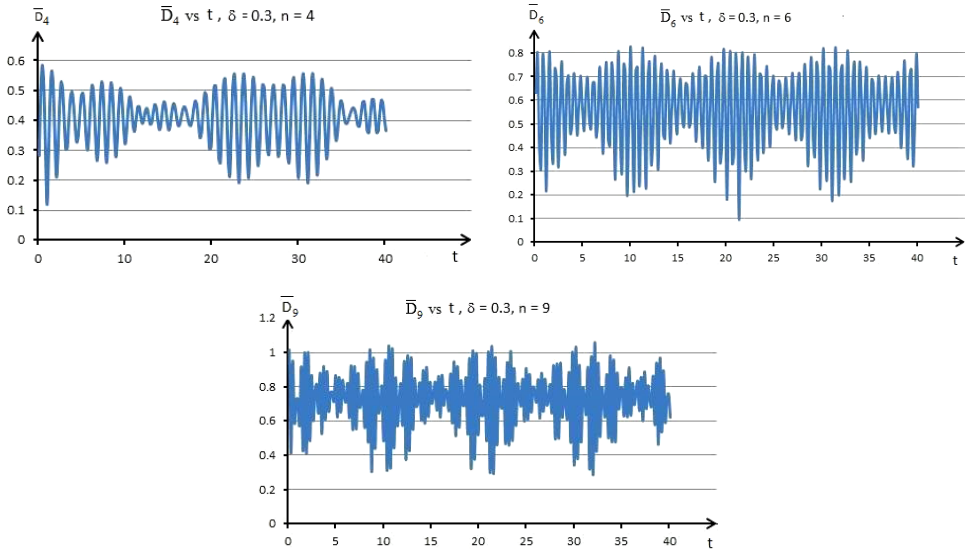

Fig. 4. $\overline{D}_n$ versus t, initial condition is the normalized projected Glauber state corresponding to the stable classical state $\mathcal{A}_2$, see (3.9), for $n = 4$, 6 and 9 bosons, $f = 5$ sites, $\delta = 0.3$.

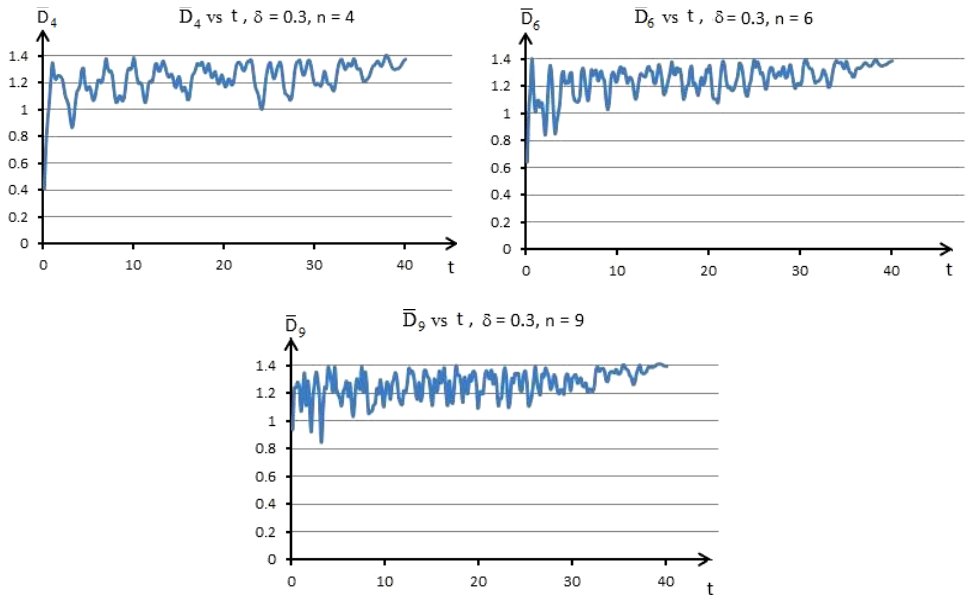

Fig. 5. $\overline{D}_n$ versus t, initial condition is the normalized projected Glauber state corresponding to unstable classical state $\mathcal{A}_3$, see (3.10), for $n = 4$, 6 and 9 bosons, $f = 5$ sites, $\delta = 0.3$.

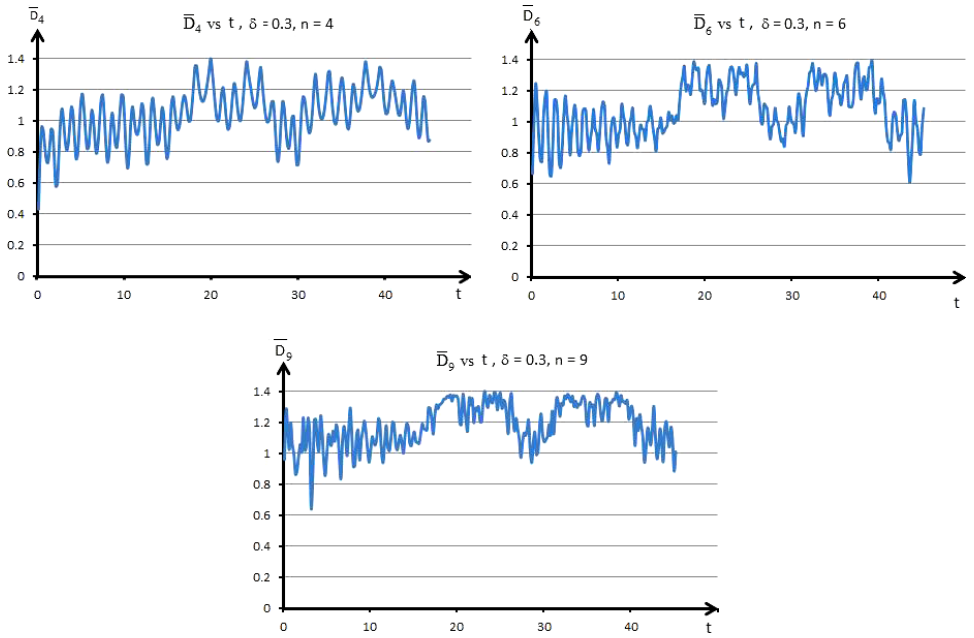

Fig. 6. $\overline{D}_n$ versus t, initial condition is the normalized projected Glauber state corresponding to unstable classical state $\mathcal{A}_4$, see (3.11), for $n = 4$, 6 and 9 bosons, $f = 5$ sites, $\delta = 0.3$.

that the classically evolved coherent state is far from the exact quantum state at all times.

Figure 6 is obtained using the coherent state corresponding to the classical initial condition $\alpha(0) = \mathcal{A}_4$, for $n = 4$, 6, and $n = 9$ bosons, respectively. The case corresponding to two consecutive peaks shows a smaller difference than the $\overline{D}_n$ above, despite being unstable. The classical solution is unstable, and the energy tends to concentrate on site 3, with a smaller amplitude at site 2 (other sites have even smaller amplitudes). This behavior is different from what was seen in the classical $f = 3$ lattice,[33] where there were recurrences to the configuration with peaks at the two consecutive sites.

Figure 7 compares $\overline{D}_n(t)$ for coherent states corresponding the classical states $\mathcal{A}_2$, and a nearby initial condition $\mathcal{A}_2{}'$, while Fig. 8 compares $\overline{D}_n(t)$ for the coherent states $\mathcal{A}_3$ and a nearby initial condition $\mathcal{A}_3{}'$. These graphs indicate the relative robustness of the above phenomena for points in the neighborhood of stable and unstable breathers, respectively.

Similar observations on the evolution of $\overline{D}_n$ were recently reported for the $f = 3$ DNLS lattice in Ref. 22. In this work, we also proposed a possible explanation of the recurrence seen for stable breathers, based on the fact that breather orbits correspond to periodic coherent states (under the alternative evolution rule). The period of this state can be compared to the quasiperiods of the exact quantum

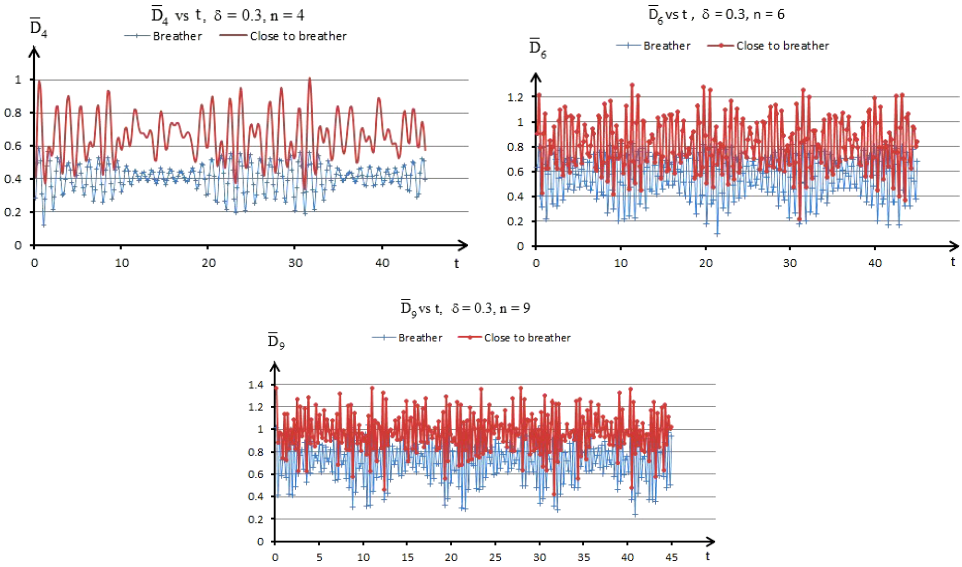

Fig. 7. Comparison of $\overline{D}_n$ versus t for initial conditions that are normalized projected Glauber states corresponding to the stable classical state $\mathcal{A}_2$, see (3.9), and $\mathcal{A}_2'$ (nearby point, $||\mathcal{A}_2 - \mathcal{A}_2'|| \sim 0.14$), for $f = 5$, $\delta = 0.3$ and $n = 4$, 6 and 9 bosons.

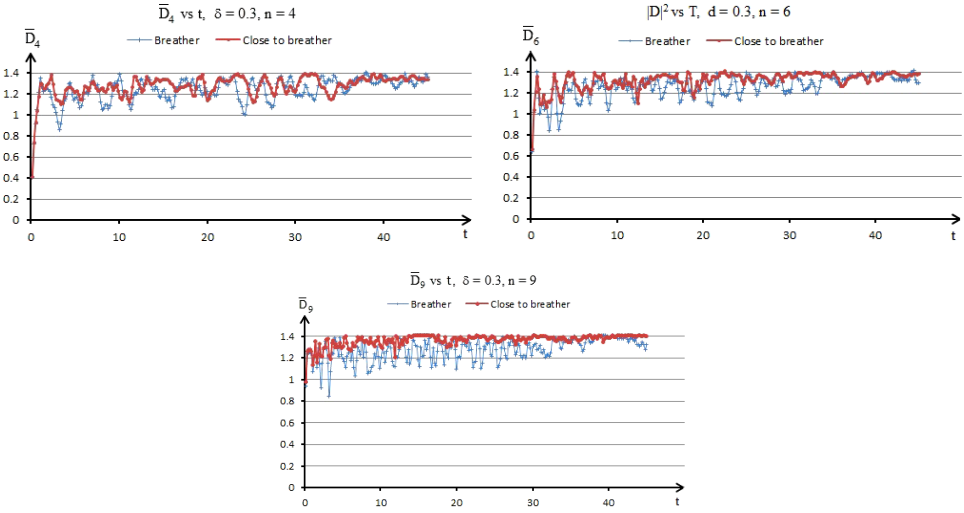

Fig. 8. Comparison of $\overline{D}_n$ versus t for initial conditions that are normalized projected Glauber states corresponding to the unstable classical state $\mathcal{A}_3$, see (3.10), and $\mathcal{A}_3'$ (nearby point with $||\mathcal{A}_3 - \mathcal{A}_3'|| \sim 0.14$) for $\delta = 0.3$ and $n = 4$, 6 and 9 bosons.

evolution in each V_n, considering also the projection of the initial coherent state to the eigenvectors of the corresponding Hamiltonian H_n. It is possible for instance that we have a reduced number of quasiperiods, up to a small error. Calculations to check this hypothesis are currently in progress.

As in Ref. 22, the stable breathers considered here are also nonlinearly (orbitaly) stable. Further work must also address the evolution from coherent states corresponding to linearly stable breathers that are not relative extrema of the energy, e.g., linearly stable multi-peak breathers.[21]

4. Discussion

We have studied numerically the distance between exact quantum states and classically evolved coherent states, using as initial conditions SU(f) coherent states corresponding to classical DNLS breather orbits and their vicinity. We used a system of five sites and presented evidence that the evolution of this distance depends on the stability of the breather solutions used. For stable breathers and their vicinity, we see that the distance shows recurrence to relatively small values of this distance. The recurrence times depend on the number of quanta. Such recurrences are not observed when we consider unstable initial conditions. Instead unstable orbits seem to correspond to large distance between the two evolutions at all times. Similar results were also seen in the $f = 3$ lattice, see Ref. 22, where we also outlined a possible explanation of the recurrences that we are investigating at present. This work in progress also aims to give an estimate of the approximate recurrence times.

Acknowledgments

We acknowledge partial support from Grants SEP-CONACyT 177246, PAPIIT IN103916 and FENOMEC.

References

1. C. Xian-Rong, G. Qing-Quan and P. Xiao-Feng, Calculation of vibrational energy spectra of H_2O molecule by nonlinear quantum theory, *Chin. Phys. Lett* **31** (1996) 660–663.
2. C. Xian-Rong, C. Yan, L. Jun, G. Qing-Quan and P. Xiao-Feng, High-lying vibrational spectrum of ammonia via nonlinear quantum theory, *Commun. Theor. Phys.* **31** (1999) 169–174.
3. C. Xian-Rong, G. Qing-Quan, P. Xiao-Feng and C. Yan, A nonlinear model for highly excited vibrational energy levels of silane, *Acta Phys. Sin.* **8** (1999) 131–135.
4. W. Z. Wang, J. T. Gammel and A. R. Bishop, Quantum breathers in a nonlinear lattice, *Phys. Rev. Lett.* **76** (1996) 3598.
5. B. I. Swanson, J. A. Brozik, S. P. Love, G. F. Strouse, A. P. Shreve, A. R. Bishop, W.-Z. Wang and M. I. Salkola, Observation of intrinsically localized modes in a discrete low-dimensional material, *Phys. Rev. Lett.* **82** (1999) 3288.
6. H. Hennig, J. Dorignac and D. K. Campbell, Transfer of Bose–Einstein condensates through discrete breathers in an optical lattice, *Phys. Rev. A* **82** (2010) 053604.
7. X. Li, Y. Wu, D. Steel, D. Gammon, T. H. Stievater, D. S. Katzer, D. Park, C. Piermarocchi and L. J. Sham, An all-optical quantum gate in a semiconductor quantum dot, *Science* **301** (2003) 809–811.
8. J. C. Eilbeck, P. S. Lomdahl and A. C. Scott, The discrete self-trapping equation, *Physica D* **16** (1985) 318–338.

9. D. N. Christodoulides and R. I. Joseph, Discrete self-focusing in nonlinear arrays of coupled waveguides, *Opt. Lett.* **18** (1988) 794.
10. P. G. Kevrekidis, *The Discrete Nonlinear Schrödinger Equation* (Springer, New York, 2009).
11. R. J. Glauber, Coherent and incoherent states of the radiation field, *Phys. Rev.* **131** (1963) 2766–2788.
12. J. C. Klauder and E. G. C. Sudarshan, *Fundamentals of Quantum Optics* (W.A. Benjamin, New York, 1968).
13. D. M. Gitman and A. L. Shelepin, Coherent states of the SU(N) groups, arXiv: hep-th/9208017v1.
14. P. Buonsante and V. Penna, Some remarks on the coherent-state variational approach to nonlinear boson models, *J. Phys. A, Math. Theor.* **41** (2008) 175301.
15. F. Trimborn, D. Witthaut and H. J. Korsch, Exact number preserving phase–space dynamics in the M-site Bose–Hubbard model, *Phys. Rev. A* **77** (2008) 043631.
16. A. C. Scott and J. C. Eilbeck, The quantized discrete self-trapping equation, *Chem. Phys. Lett.* **132** (1986) 23.
17. L. Bernstein, J. C. Eilbeck and A. C. Scott, The quantum theory of local modes in a coupled system of nonlinear oscillators, *Nonlinearity* **3** (1990) 293–323.
18. D. Ellinas, M. Johansson and P. L. Christiansen, Quantum nonlinear lattices and coherent state vectors, *Physica D* **34** (1999) 126–143.
19. R. S. MacKay and S. Aubry, Proof of existence of breathers for time-reversible or Hamiltonian networks of weakly coupled oscillators, *Nonlinearity* **7** (1994) 1623–1643.
20. M. I. Weinstein, Excitation thresholds for nonlinear localized modes on lattices, *Nonlinearity* **12** (1999) 673–691.
21. D. E. Pelinovsky, P. G. Kevrekidis and D. J. Frantzeskakis, Stability of discrete solitons in nonlinear Schrödinger lattices, *Physica D* **212** (2005) 1–19.
22. R. Martínez-Galicia and P. Panayotaros, Localization and coherent states in a quantum DNLS trimer, *Eur. Phys. J. - S. T.* **225** (2016) 2717.
23. L. Amico and V. Penna, Dynamical mean field theory of the Bose–Hubbard model, *Phys. Rev. Lett.* **80** (1998) 2189.
24. A. G. Basile and V. Elser, Equations of motion for superfluids, *Phys. Rev. E* **51** (1995) 5688.
25. S. Raghavan, A. Smerzi and V. M. Kenkre, Transitions in coherent oscillations between two trapped Bose–Einstein condensates, *Phys. Rev. A* **60** (1999) 1787.
26. F. Trimborn, D. Witthaut and H. J. Korsch, Beyond mean-field dynamics of small Bose–Hubbard systems based on the number-conserving phase–space approach, *Phys. Rev. A* **79** (2009) 013608.
27. M. Hiller, T. Kottos and T. Geisel, Wave-packet dynamics in energy space of a chaotic trimeric Bose–Hubbard system, *Phys. Rev. A* **79** (2009) 023621.
28. P. Buonsante, R. Franzosi and V. Penna, Dynamical instability in a trimeric chain of interacting Bose–Einstein condensates, *Phys. Rev. Lett.* **90** (2003) 050404.
29. M. Johansson, Hamiltonian Hopf bifurcations in the discrete nonlinear Schrödinger trimer: Oscillatory instabilities, quasi-periodic solutions and a 'new' type of self-trapping transition, *J. Phys. A, Math. Gen.* **37** (2004) 2201–2222.
30. T. Kapitula, P. G. Kevrekidis and Z. Chen, Three is a crowd: Solitary waves in photorefractive media with three potential wells, *SIAM J. Appl. Dyn. Syst.* **5** (2007) 598–633.
31. R. Goodman, Hamiltonian Hopf bifurcations and dynamics of NLS/GP standing-wave modes, *J. Phys. A, Math. Theor.* **44** (2011) 425101.

32. P. Panayotaros, Continuation and bifurcations of breathers in a finite discrete NLS equation, *Discrete Contin. Dyn. Syst. S* **4** (2011) 1227–1245.
33. P. Panayotaros, Instabilities of breathers in a finite NLS lattice, *Physica D* **241** (2012) 847–856.
34. P. D. Miller, A. C. Scott, J. Carr and J. C. Eilbeck, Binding energies for discrete nonlinear Schrödinger equations, *Phys. Scr.* **44** (1991) 509–516.
35. E. Wright, J. C. Eilbeck, M. H. Hays, P. D. Miller and A. C. Scott, The quantum discrete self-trapping equation in the Hartree approximation, *Physica D* **69** (1993) 18–32.
36. A. Chefles, Nearest-neighbor level spacings for the non-periodic discrete nonlinear Schrödinger equation, *J. Phys. A, Math. Gen.* **29** (1996) 4515–4526.
37. S. Flach and V. Fleurov, Tunnelling in the nonintgrable trimer-a step towards quantum breathers, *J. Phys.*: *Condens. Matter* **9** (1997) 7039–7061.
38. J. C. Eilbeck and F. Palmero, Trapping in quantum chains, *Phys. Lett. A* **331** (2004) 201–208.
39. R. A. Pinto, M. Haque and S. Flach, Edge-localized states in quantum one-dimensional lattices, *Phys. Rev. A* **79** (2009) 052118.
40. P. Buonsante, V. Penna and A. Vezzani, Quantum signatures of the self-trapping transtion in attractive lattice bosons, *Phys. Rev. A* **82** (2010) 043615.
41. R. Franzosi, S. M. Giampaolo and F. Iluminati, Quantum localization and bound-state formation in Bose–Einstein condensates, *Phys. Rev. A* **82** (2010) 063620.